Journal of Visualized Experiments

3D imaging of soft-tissue samples using an X-ray specific staining method and nanoscopic computed tomography

--Manuscript Draft--

Article Type:	Invited Methods Article - JoVE Produced Video
Manuscript Number:	JoVE60251R1
Full Title:	3D imaging of soft-tissue samples using an X-ray specific staining method and nanoscopic computed tomography
Keywords:	X ray staining method, microscopic X ray computed tomography, nanoscopic X ray computed tomography, non destructive, multiscale imaging, high resolution, 3D imaging, soft tissue imaging, microstructure, eosin stain, cytoplasm specific staining
Corresponding Author:	Madleen Busse Technical University of Munich Garching, GERMANY
Corresponding Author's Institution:	Technical University of Munich
Corresponding Author E-Mail:	madleen.busse@tum.de
Order of Authors:	Madleen Busse
	Mark Müller
	Melanie A. Kimm
	Simone Ferstl
	Sebastian Allner
	Klaus Achterhold
	Julia Herzen
	Franz Pfeiffer
Additional Information:	
Question	**Response**
Please indicate whether this article will be Standard Access or Open Access.	Open Access (US$4,200)
Please indicate the **city, state/province, and country** where this article will be **filmed**. Please do not use abbreviations.	Garching, Bavaria in Germany

TITLE:

3D Imaging of Soft-Tissue Samples using an X-Ray Specific Staining Method and Nanoscopic Computed Tomography

AUTHORS & AFFILIATIONS:

Madleen Busse[1,*], Mark Müller[1,*], Melanie A Kimm[2], Simone Ferstl[1], Sebastian Allner[1], Klaus Achterhold[1], Julia Herzen[1], and Franz Pfeiffer[1,2]

[1]Department of Physics and Munich School of BioEngineering, Technical University of Munich, Garching, Germany

[2]Department of Diagnostic and Interventional Radiology, School of Medicine and Klinikum rechts der Isar, Technical University of Munich, Munich, Germany

*These authors contributed equally.

Corresponding Author:
Madleen Busse
madleen.busse@tum.de

Email Addresses of Co-authors:
Mark Müller (mark_mueller@ph.tum.de)
Melanie A Kimm (melanie.kimm@tum.de)
Simone Ferstl (simone.ferstl@tum.de)
Sebastian Allner (sebastian.allner@tum.de)
Klaus Achterhold (klaus.achterhold@tum.de)
Julia Herzen (julia.herzen@tum.de)
Franz Pfeiffer (franz.pfeiffer@tum.de)

KEYWORDS:

X-ray staining method, microscopic X-ray computed tomography, nanoscopic X-ray computed tomography, non-destructive, multiscale imaging, high-resolution, 3D imaging, soft tissue imaging, microstructure, eosin stain, cytoplasm-specific staining

SUMMARY:

A protocol for 3D visualization of microscopic tissue structures by using an X-ray specific staining method designed for X-ray computed tomography is presented.

ABSTRACT:

We demonstrate a laboratory-based method combining X-ray microCT and nanoCT with a specific X-ray stain, which targets the cell cytoplasm. The described protocol is easy to apply, fast and suitable for larger soft-tissue samples. The presented methodology enables the characterization of crucial tissue structures in three dimensions and is demonstrated on a whole mouse kidney. The multiscale approach allows to image the entire mouse kidney and supports the selection of further volumes of interest, which are acquired with higher resolutions ranging into the

nanometer range. Thereby, soft-tissue morphology with a similar detail level as the corresponding histological light microscopy images is reproduced. Deeper insights into the 3D configuration of tissue structures are achieved without impeding further investigations through histological methods.

INTRODUCTION:

Full characterization of soft-tissue specimens requires information about the 3D tissue microstructure. The current gold standard for soft-tissue sample analyses is histopathology. The tissue and cellular morphology of the specimen are explored in 2D within selected regions of interest (ROIs) using optical microscopy[1]. This method, however, has several drawbacks. The preparation of the sample is time-consuming, complicated, destructive and prone to artifacts. The produced microscopic slides provide only 2D information parallel to the sectioning plane. Often the number of histological sections, which are investigated, is restricted due to time constraints[2,3].

In recent years, the field of 3D histology has evolved. Here, virtual tissue slices from any desired spatial plane are accessible. This allows for the tracking of structures throughout the sample, which leads to a deeper understanding of the 3D tissue architecture and structural changes associated with different pathologies. Various methods have been developed to achieve the generation of 3D volume data. They range from serial-section based approaches, which use either light or electron microscopy[4-8], to block-face imaging methods, such as episcopic 3D imaging or block-face scanning electron microscopy[7-9]. All the mentioned methods, however, involve either sectioning or destruct the sample completely, which does not allow for further investigations. The obtained resolution is highly dependent on the sectioning process being prone to artifacts as described in conventional histology. These methods suffer also from alignment artifacts.

3D X-ray imaging techniques such as microscopic and nanoscopic computed tomography (microCT and nanoCT) aspire to generate 3D high-resolution data without destruction of the tissue sample. So far, the weak X-ray attenuation contrast of soft tissue and the limited access to high resolutions in a laboratory environment has impaired their use for 3D visualization of microscopic tissue structures. Recent advances towards laboratory-based, high-resolution X-ray CT allow for resolutions well below 1 µm [10-13].

The lack of contrast in soft tissue in conventional attenuation-based X-ray imaging is compensated by staining agents, which enhance the X-ray attenuation contrast. Staining agents known from other imaging techniques such as osmium tetroxide (OsO_4), iodine potassium iodide (IKI) or phosphotungstic acid (PTA) are often used[14-25]. Staining agents that allow for (i) specific biological targeting, (ii) homogenous and complete staining, (iii) easy handling, (iv) fast penetration of the tissue without creating artifacts such as diffusion rings, (v) large and dense tissue staining, and (vi) full compatibility with histopathology are required to establish X-ray CT as tool for 3D visualization of microscopic tissue structures. In this work, we show how soft-tissue samples are prepared for X-ray CT imaging with a cytoplasm-specific X-ray stain based on eosin that fulfills the requirements stated above[26].

The multiscale imaging approach ensures the assessment of staining quality through an overview microCT measurement and the selection of volumes of interest (VOIs) for further high-resolution investigations. Staining quality is analyzed focusing on staining parameters such as (i) completeness, (ii) appearance of diffusion rings, (iii) contrast enhancement, (iv) appearance of CT artifacts such as streaks and (v) homogeneity. The laboratory-based nanoCT setup, which uses geometric magnification to reach resolutions down to 100 nm, visualizes soft-tissue morphology on (sub)-cellular level[10,27]. A comparative analysis of the nanoCT slices with corresponding histological light microscopy images confirms the reproduction of tissue architecture with similar detail on a microscopic level in 2D, enabling histopathological characterization of the tissue sample. This detailed video protocol is intended to raise the awareness and to highlight the potential of this methodology as non-destructive 3D soft-tissue imaging tool being of interest to a wide scientific community such as zoologists, biologists and health professionals.

PROTOCOL:

Caution: Please consult all relevant material safety data sheets (MSDS) before use. Several of the chemicals used in the protocol are acutely toxic and carcinogenic. Please use all appropriate safety practices when performing the staining protocol including the use of engineering controls (fume hood, glovebox) and personal protective equipment (safety glasses, gloves, lab coat, full length pants, closed-toe shoes).

Animals Used:

Animal housing was carried out at the Klinikum rechts der Isar, Technical University of Munich in accordance with the European Union guidelines 2010/63. Organ removal was approved from an internal animal protection committee of Klinikum rechts der Isar, Munich, Germany (internal reference number 4-005-09). All procedures were in accordance with relevant guidelines and regulations. All laboratories are inspected for accordance with the OECD principles of good laboratory practice.

1. Eosin staining protocol

1.1 To fixate soft-tissue samples, fill a 50 mL centrifuge tube with a fixative solution containing 9.5 mL of 4% (v/v) formaldehyde solution (FA) and 0.5 mL of glacial acetic acid (AA).

NOTE: Prepare the FA solution freshly from a 37% acid free FA solution stabilized with approximate 10% methanol. Dilute the FA solution further with Dulbecco's phosphate buffered saline (DPBS). Choose DPBS without calcium and magnesium. Keep the dilute FA solution no longer than one month. During acidification the pH of the fixative solution is changing from neutral to approximately 3.

CAUTION: Because FA is acute organ toxic, corrosive and carcinogenic, the use of a fume hood is mandatory and appropriate protective personal equipment must be used.

1.1.1 Add the freshly removed soft-tissue sample to a 50 mL centrifuge tube and refrigerate the 50 mL centrifuge tube for 24-72 h.

NOTE: The protocol can be paused here.

1.1.2 Wash the soft-tissue sample with DPBS solution for 1 h.

1.2 To stain the fixated soft-tissue sample (e.g., a whole mouse kidney), place the soft tissue in 2 mL of eosin Y-staining solution and incubate the sample for 24 h. Keep the sample on a horizontal shaking plate for a smooth rocking (ca. 60 rpm) during the incubation process.

NOTE: The eosin Y-staining solution has a concentration of 30% (w/v) in distilled water. Choose the volume of the staining solution in such a way that the sample is completely covered by the staining solution and allow the sample to move freely within the sample container. The incubation time may differ for other samples and has to be adjusted accordingly.

1.3 After staining, remove the soft tissue sample carefully from the sample container.

1.3.1 Carefully remove excess of staining agent with cellulose tissue paper.

1.3.2 Place the soft-tissue sample in a conical sample container above an ethanol vapor phase for storage and further use.

NOTE: The conical sample container must always contain a few drops of 70% (v/v) ethanol at the bottom of the tube to keep the soft-tissue sample moist and prevent artifacts.

2 X-ray microCT imaging

NOTE: The X-ray microCT measurements were performed with a microCT scanner, which offers overview CT measurements (the ability to image the entire sample within the field of view (FOV)) and the performance of high-resolution CT measurements (the ability to focus in on one desired volume of interest (VOI) of the very same sample) down to 1 µm.

2.1 Mount the soft-tissue sample to an appropriate sample holder. Ensure a tight fit of the sample on the sample holder to prevent the sample from moving during the X-ray CT measurements.

2.1.1. In case of the stained mouse kidney: Prepare a sample holder with two centrifuge tubes, whereby the bottom of one tube is cut off. Glue the two centrifuge tubes together using two-component adhesive. Ensure a straight alignment of the centrifuge tubes around the rotation axis. Wait for the adhesive to harden.

2.1.2. Once the sample holder is ready for use, transfer the mouse kidney into the intact

centrifuge tube, which holds a few drops of 70% (v/v) ethanol at the bottom of the tube.

NOTE: Stability of the sample is crucial. Take time to prepare the sample for X-ray CT measurements. The soft-tissue sample is kept over an ethanol vapor phase to keep the sample moist during the X-ray CT measurements and prevent the soft-tissue sample from shrinkage and other artifacts. The soft-tissue sample should not be in contact with the solvent to obviate accumulation of the solvent around the sample during X-ray CT measurement, which might lead to sample movement during the measurement or might cause problems during reconstruction. If the sample holder does not allow to hold solvent at the bottom, a cellulose paper moistened with 70% (v/v) ethanol can be placed in the sample holder. It should be noted that shrinkage artifacts due to the solvent ethanol were not observed.

The protocol can be paused here.

2.2 After careful alignment of the sample, choose acquisition parameters for best image quality. In case of the presented microCT data, acquire the scan at a peak voltage of 50 kV, a current of 3.5 W using 1601 projections equally distributed over 360°.

NOTE: The acquisition parameters for the overview CT scan were chosen for best image quality. As such the 0.39x camera objective was chosen to cover the whole sample within the field of view (FOV). This resulted in an effective pixel size of 12 µm. The exposure time of 2 s per projection provided a good signal to noise ratio. The ROI for the high-resolution CT scan was identified using the microCT data from the overview scan. MicroCT scanners often incorporate an integrated software tool, which allows for the precise selection of the determined ROI. For the high-resolution CT data, the 4x camera objective was chosen resulting in an effective pixel size of 3.3 µm. Here, an exposure time of 15 s per projection was needed.

The protocol can be paused here.

2.3 After acquisition of the X-ray CT data, process the projections accordingly for reconstruction of the 3D volume. In case of the presented microCT data: Reconstruct the X-ray CT data with the integrated software.

NOTE: The volume renderings of the microCT data shown in **Figure 1 and Figure 2** were generated using a visualization software.

The protocol can be paused here.

3 X-ray nanoCT imaging

NOTE: The X-ray nanoCT scanner has been developed in-house. The lens-free instrument is equipped with a nanofocus X-ray source and a single-photon counting detector. 3D data with resolutions down to 100 nm can be generated[10]. Generally, nanoCT systems including those with X-ray optics are commercially available and not limited to the described nanoCT scanner.

3.1 NanoCT sample preparation

3.1.1 Prepare VOIs of the soft-tissue sample. Cut the soft tissue into very small pieces of approximately 0.5 mm edge length using a scalpel and a stereomicroscope. In case of the mouse kidney: Cut the mouse kidney into two halves along the longest axis. Take one half of the mouse kidney and prepare different anatomical regions such as renal cortex and renal medulla.

NOTE: The other halve of the mouse kidney was transferred to histopathology, where the sample was embedded into paraffin and processed accordingly to yield the typical histological sections as seen in **Figure 3c** and **Figure 3d**.

3.1.2 Transfer the small pieces before the first dehydration step to a new Petri dish, where they remain for all subsequent steps.

3.1.3 Dehydrate the samples using concentrations (all v/v) in %: 50, 60, 70, 80, 90, 96 and 100 ethanol balanced with distilled water. Perform each dehydration step for 1 h each.

NOTE: The protocol can be paused here. Keep the small tissue pieces in 100% ethanol overnight.

3.1.4 Critical point dry (CPD) the small tissue pieces.

NOTE: The application of CPD enables the complete dehydration of the tissue sample by exchanging the solvent (here ethanol) with the drying agent (here CO_2). This has been necessary to ensure that the sample can be mounted to the sample holders of the nanoCT, is not moving during the measurement and can be positioned very close to the X-ray source to allow for best geometrical magnification. The nanoCT setup is based on mere geometrical magnification, with the magnification factor being defined as the source-to-detector distance over the source-to-sample distance. The drying technique was first introduced by Anderson to preserve the 3D structure of biological specimens for electron microscopy[33]. An overview of the technique is provided by Bray[34].

3.1.4.1 Prefill the vacuum chamber with 100% ethanol. Transfer the small tissue pieces into a silicon basket and place the basket in the vacuum chamber of the CPD. Close the system.

NOTE: Since high pressure is involved in the CPD process, ensure all parts of the CPD, in particular the fittings, are intact and the system is properly closed.

3.1.4.2 Cool the chamber to 6- 8°C and fill up with liquid CO_2.

3.1.4.3 While stirring, wait 3 min to allow for proper mixing of the two components. Carefully drain the chamber. Ensure the sample holder is still covered with solvent. Repeat this step ten times to allow complete replacement of ethanol with CO_2 within the sample.

3.1.4.4 After the final filling of the chamber with CO_2, heat the machine to the critical point of CO_2 (31 °C and 73.8 bar) followed by very slow release of the gaseous CO_2 over a time of 30 min.

NOTE: The release of the gas should be undertaken very slowly as otherwise condense water can form on the sample. Ensure that the temperature does not drop below the critical point of CO_2. Only open the CPD machine when all pressure has been released from the system.

3.1.4.5 Remove the CPD tissue pieces quickly from the machine and keep them in a new Petri dish stored in a desiccator prior to further use.

NOTE: The protocol can be paused here.

3.2 Mount the CPD tissue pieces to an appropriate sample holder. Ensure a tight fit of the sample on the sample holder to prevent the sample from moving during the CT measurements. In case of the CPD mouse kidney tissue pieces: Glue the tissue pieces with superglue to a sample holder.

NOTE: Any undesired movement of the sample during CT measurements can cause problems during volume reconstruction - especially when acquiring a data set with nanometer voxel size.

The protocol can be paused here.

3.3 After careful alignment of the sample, choose acquisition parameters for best image quality. In case of the presented nanoCT data: Acquire projections at a peak voltage of 60 kV with 1599 projections equally distributed over 360° and a voxel size of approximately 400 nm.

NOTE: A single CT measurement acquired at 400 nm voxel size has a FOV of 75 µm in the direction of the rotation axis (vertical) and approximately 560 µm in the direction perpendicular to the rotation axis (horizontal). To investigate larger volumes, an extension of the FOV along the rotation axis can be achieved by combining multiple scans at different vertical positions. Additionally, local tomography scans can be performed to measure samples with a larger sample diameter perpendicular to the rotation axis than given by the FOV of a global CT scan. The nanoCT data was acquired with an exposure time of 4 s per projection. As such the total acquisition time per data set was approximately 3.5 h.

The protocol can be paused here.

3.4 After acquisition of the CT data, process the projections accordingly for reconstruction of the 3D volume.

3.4.1. In case of the presented nanoCT data, normalize the acquired projections with flat-field images. Enhance the sharpness of the projections by using a Richardson-Lucy deconvolution algorithm[35,36]. Use a rotationally symmetric Gaussian function with a standard deviation of one pixel as deconvolution kernel.

3.4.2. Apply Paganin's phase-retrieval algorithm to the sharpened images to increase the soft-tissue contrast. Set the parameters of the algorithm to optimize the image quality[37]. Reconstruct the pre-processed projections with a state-of-the-art filtered backprojection algorithm.

NOTE: **Figure 3** evaluates the obtained nanoCT data with corresponding histological sections, which were approximately 7 µm thick. Therefore, minimum intensity projection slices of 18 adjacent nanoCT slices with a virtual thickness of approximately 7 µm were generated by means of calculating the minimum value for each pixel in the relevant slices. A visualization software was used to render the volume of the nanoCT data, which is displayed in **Figure 4**.

REPRESENTATIVE RESULTS:

Figure 1 shows CT slices and volume rendering of low-resolution microCT data highlighting contrast enhancement after staining. **Figure 2** shows CT slices and volume rendering of high-resolution microCT data derived from a local tomography of the whole mouse kidney. **Figure 3** shows CT slices of nanoCT data in comparison to the corresponding histological sections. **Figure 4** shows CT slice and volume rendering of nanoCT data highlighting structural details at cellular level. The low-resolution microCT measurement allows for an overview of the whole organ and helps to identify volumes of interest (VOIs) for the high-resolution microCT measurement. Through this multiscale approach, the VOI for the nanoCT is determined. The nanoCT enables a very detailed view of the soft-tissue sample on cellular level. The comparative study with the corresponding histological section highlights full compatibility with histopathology. Here, the multimodal imaging approach is confirming the results obtained with both modalities.

FIGURE AND TABLE LEGENDS:

Figure 1. CT slices and volume rendering of the low-resolution microCT data. (**a**,**b**) Overview images of the same mouse kidney before and after staining, respectively, highlighting the contrast enhancement obtained after application of the eosin-based staining protocol. Both microCT data sets were acquired using identical acquisition parameters. The voxel size in both data sets is 12 µm. The contrast enhancement achieved in (**b**) enables the identification of the following anatomic structural regions: Cortex (I), outer medulla (II) with further distinction in outer stripes of outer medulla (IIa) and inner stripes of outer medulla (IIb), inner medulla (III), papilla (IV) and renal pelvis (V). (**c**) Volume rendering of microCT data showing a virtual sagittal section through the whole mouse kidney. This figure has been modified from Busse and Müller et al.[26]

Figure 2. CT slice and volume rendering of high-resolution microCT data derived from the same mouse kidney after application of the developed eosin-based staining protocol. (**a**) The left corner shows the overview microCT image highlighting the ROI (blue box) for the displayed high-resolution image. The following anatomic structural regions are identifiable: Cortex (I), outer medulla (II) with further distinction in outer stripes of outer medulla (IIa) and inner stripes of outer medulla (IIb), inner medulla (III), minor calyx (IV) and vessels (V and VI). (**b**) Volume of interest rendering of the high-resolution microCT data acquired with a voxel size of 3.3 µm. The

medulla region and a virtual section through a vessel derived from a local tomography of the whole kidney. This figure has been modified from Busse and Müller et al.[26].

Figure 3. CT slices of nanoCT data (a,b) in comparison to the histological sections (c,d) derived from the same mouse kidney after application of the developed eosin-based staining protocol. (**a**) The nanoCT image of the same mouse kidney sample after staining, dissecting and CPD shows detailed structures of region (IIb) seen in **Figure 1 and 2**. These are known as thick ascending limbs of the loop of Henle. (**b**) Minimum intensity projection slice derived from the same nanoCT data set shown in (**a**) with a virtual slice thickness of approximately 7 µm, which allows for clear visualization of the cell nuclei. (**c**) Representative histological section displaying thick ascending limbs of the loop of Henle with clear visualization of cell nuclei and brush border. The histological section has an approximate thickness of 7 µm and was obtained from the same mouse kidney sample after the applied eosin-based staining and embedding in a paraffin block. (**d**) Representative histological section with application of counter stain hematoxylin highlighting the cell nuclei in purple. Preparation of the histological section close to the section shown in (**c**) with approximate thickness of 7 µm. This figure has been modified from Busse and Müller et al.[26]

Figure 4. CT slice and volume rendering of nanoCT data. (**a**) The nanoCT image of the same mouse kidney sample showing the structures known as thick ascending limbs of the loop of Henle. This is a detailed view of region (IIb) seen in **Figure 1 and 2** acquired from a small piece of the kidney with a voxel size of approximately 400 nm. The preparation of the sample involved staining, dissecting and CPD. (**b**) Volume rendering of nanoCT data visualizing the 3D structure of thick ascending limbs of the loops of Henle. This figure has been modified from Busse and Müller et al.[26]

DISCUSSION:

Currently, eosin is used as the standard histological protocol to label the cell cytoplasm. The staining agent is applied as a 0.1% (w/v) aqueous solution to microscopic slices of soft tissue (generally cut with a thickness of 2-10 µm)[38]. The application of this standardized histological protocol to 3D tissue samples such as a whole mouse kidney does not result in an attenuation contrast enhanced CT image. On the one hand, this can be attributed to the low intrinsic attenuation properties of soft tissue for typically used X-ray energies of laboratory-based microCT systems. Usually, soft tissue is composed of mainly carbon, hydrogen, oxygen and nitrogen[39], and therefore, does not result in contrast enhancement. On the other hand, the low concentration of eosin used for staining was the limiting factor. Even though one eosin molecule holds four bromide atoms (high atomic number element bromine with Z = 35[39]), the sensitivity levels required for X-ray CT imaging were not met.

To overcome this challenge of low attenuation contrast, several concentrations of eosin were investigated. A limitation is here the maximum solubility of eosin in water, which is 30% (w/v) in an aqueous solution. Best attenuation contrast enhancement within the soft tissue was observed with the highest eosin concentration, which was expected according to the Lambert-Beer Law. Therefore, the final staining protocol was carried out with the highest concentration.

The question how to prepare the soft tissue optimally on a molecular level for the staining procedure to further improve contrast enhancement was answered by pH adjustment. Here, the acidification of the soft-tissue sample during fixation or before staining was found to be crucial. This was also shown by Hong et al.[40]. The higher accumulation of staining agent within the cell cytoplasm by the acid was achieved through improved ionic interactions, which were a result of the protonation of amino acid side chains of proteins and peptides present within the cell cytoplasm. A representative result highlighting the contrast enhancement in comparison to an unstained soft-tissue sample is shown in **Figure 1a and 1b**. Here, a structural overview of a whole mouse kidney visualizing crucial anatomical regions such as cortex, medulla, papilla and renal pelvis was achieved.

The presented staining protocol is simple to apply and contains only three steps. The required reagents are easily accessible. The overall staining time of 24 hours is fast for a whole-organ staining, which enables the 3D visualization of soft-tissue samples (**Figure 1c, 2b and 4b**) in a laboratory environment at multiple scales down to cellular level. It should be noted that the overall staining time and volume of the staining solution needed might request some adaptations depending on the nature of the sample. Nevertheless, the eosin-based staining protocol is suitable for whole-organ staining, which then enables high-resolution microCT imaging of whole organs. Shrinkage artifacts due to the solvent ethanol, which was used to keep the sample moist during the microCT measurements, were not observed. Additional preparation steps are required for nanoCT imaging, which allows for the investigation of smaller tissue pieces retrieved from the original sample. With respect to future histopathological applications, the overview scans will provide valuable insights into altered anatomical regions and structures, which allow for the determination of ROIs as demonstrated in **Figure 2a**. Those can be studied in 3D by microCT (**Figure 1c and 2b**) or nanoCT (**Figure 4b**) and evaluated in 2D with histology (**Figure 3**).

Another strength of the protocol is seen in the full compatibility with histopathology with respect to the H&E staining procedure. The application of the eosin-based staining procedure to bulk samples does not impede further histological investigations (**Figure 3**), even though the applied eosin concentration is much higher compared to the histological staining solution. The nanoCT slice with a virtual thickness of approximately 400 nm (**Figure 3a**) compares already very well with the histological section (**Figure 3c**), which was derived from the corresponding soft-tissue sample. Considering the approximate thickness of a histological section with 7-10 µm, the generation of minimum intensity projection slices of the nanoCT data (**Figure 3b**), which correspond to a virtual thickness of approximately 7 µm, allows for a better comparison with the histological section (**Figure 3c**). Here, the cell nuclei are clearly revealed as non-attenuation area as eosin specifically stains proteins and peptides in the cell cytoplasm[38].

The application of further counter staining with standard histological methods is possible, even though the order of the staining compared to the standard histological staining procedure was reversed. Starting first with the developed eosin-based staining protocol for CT, followed by counter staining of those eosin-based histological sections with hematoxylin, allows for full compatibility and results in a high-quality staining displaying the expected form of appearance. The cell nuclei-specific staining with Mayer's sour hematoxylin was applied to the histological

section highlighting the cell nuclei in purple (**Figure 3d**). The application of histological counter staining is currently limited to the H-stain. Other standard histological counter stainings such as periodic acid Schiff's base, Elastica van Gieson or Gomorri silver have to be evaluated as well as the compatibility with immunohistological techniques needs to be tested.

The eosin-based staining protocol allows for (i) cell cytoplasm-specific targeting, (ii) homogenous and complete staining, (iii) easy implementation, (iv) fast penetration of the tissue without creating artifacts such as diffusion rings, (v) the staining of large and dense soft-tissue samples, and (vi) full compatibility with histopathology in respect of the H&E stain. These requirements are important to allow high-resolution X-ray CT visualization of soft tissue down to cellular level. In combination with the recently developed nanoCT devices[12,28,32,41-44], non-destructive generation of virtual histological slices that are comparable in contrast and resolution to conventional histological data is rendered possible. This combined approach will enable the establishment of X-ray CT as a valuable tool for the 3D visualization of microscopic tissue structures.

ACKNOWLEDGMENTS:

We thank Dr. Enken Drecoll for histological discussions and the extremely helpful team at Excillum AB, Sweden. We acknowledge financial support through the DFG Cluster of Excellence Munich Center for Advanced Photonics (MAP) and the DFG Gottfried Wilhelm Leibniz Program. Furthermore, this research project has received funding from the European's Union Horizon 2020 research and innovation program under the Marie Skłodowska-Curie Grant Agreement No. H2020-MSCA-IF-2015-703745-CONSALT.

DISCLOSURES:

The authors have nothing to disclose.

REFERENCES:

1 Suvarna, S. K., Layton, C., Bancroft, J. D. *Theory and Practice of Histological Techniques*. 7th edn, (Churchill Livingstone Elsevier, 2013).

2 Chatterjee, S. Artefacts in histopathology. *Journal of Oral and Maxillofacial Pathology.* **18** (4), 111-116 (2014).

3 McInnes, E. Artefacts in histopathology. *Comparative Clinical Pathology.* **13** (3), 100-108 (2005).

4 Andreasen, A., Drewes, A., Assentoft, J., Larsen, N. Computer-assisted alignment of standard serial sections without use of artificial land-marks. A practical approach to the utilization of incomplete information in 3-d reconstruction of the hippocampal region. *Journal of Neuroscience Methods.* **45** (3), 199-207 (1992).

5 Braverman, M. S., Braverman, I. M. Three-dimensional reconstructions of objects from serial sections using a microcomputer graphics system. *Journal of Investigative Dermatology.* **86** (3), 290-294 (1986).

6 Denk, W., Hortsmann, H. Serial block-face scanning electron microscopy to reconstruct three-dimensional tissue nanostructure *PLoS Biology.* **2** (11), e329 (2004).

7 Mohun, T. J., Weninger, J. W. Imaging heart development using high-resolution episcopic

microscopy. *Current Opinion in Genetics and Development.* **21**, 573-578 (2011).
8 Weninger, J. W., Meng, S., Streicher, J., Müller, G. B. A new episcopic method for rapid 3-d reconstruction: applications in anatomy and embryology. *Anatomy and Embryology.* **197** (5), 341-348 (1998).
9 Odgaard, A., Andersen, K., Melsen, F., Gundersen, H. J. G. A Direct Method for Fast 3-Dimensional Serial Reconstruction. *Journal of Microscopy.* **159**, 335-342 (1990).
10 Müller, M. et al. Myoanatomy of the velevt worm leg revealed by labratory-based nanofocus X-ray source tomography. *Proceedings of the National Academy of Sciences of the United States of America.* **114** (47), 12378-12383 (2017).
11 Salomon, M., Hanke, R., Krüger, P., Uhlmann, N., Voland, V. Realization of a computed tomography setup to achieve resolutions below 1 µm. *Nuclear Instruments and Methods in Physics Research Section A.* **591**, 50-53 (2008).
12 Tkachuk, A. et al. X-ray computed tomography in Zernike phase contrast mode at 8 keV with 50-nm resolution using Cu rotating anode X-ray source. *Zeitschrift für Kristallographie.* **222**, 650-655 (2007).
13 Withers, P. J. X-ray nanotomography. *Materials Today.* **10**, 26-34 (2007).
14 Jahn, H. et al. Evaluation of contrasting techniques for X-ray imaging of velvet worms (Onychophora). *Journal of Microscopy.* **270** (3), 343-358 (2018).
15 Martins de S. e Silva, J. et al. Three-dimensional non-destructive soft-tissue visualization with X-ray staining micro-tomography. *Scientific Reports.* **5**, 14088 (2015).
16 Metscher, B. D. MicroCT for Developmental Biology: A Versatile Tool for High-Contrast 3D Imaging at Histological Resolutions. *Developmental Dynamics.* **238**, 632-640 (2009).
17 Metscher, B. D. MicroCT for comparative morphology: simple staining methods allow high-contrast 3D imaging of diverse non-mineralized animal tissues. *BMC Physiology.* **9**, 11 (2009).
18 Mitzutani, R. et al. X-Ray Microtomographic Imaging of Three-Dimensional Structure of Soft Tissues. *Tissue Engineering Part C: Methods.* **14** (4), 359-363 (2008).
19 Pauwels, E., Loo, D. v., Cornillie, P., Brabant, L., Hoorebeke, L. v. An exploratory study of contrast agents for soft tissue visualization by means of high resolution X-ray computed tomography imaging. *Journal of Microscopy.* **250**, 21-31 (2013).
20 Degenhardt, K., Wright, A. C., Horng, D., Padmanabhan, A., Epstein, J. A. Rapid 3D phenotyping of cardiovascular development in mouse embryos by micro-CT with iodine staining. *Circulation: Cardiovascular Imaging.* **3** (3), 314-322 (2010).
21 Dullin, C. et al. µCT of ex-vivo stained mouse hearts and embryos enables a precise match between 3D virtual histology, classical histology and immunochemistry. *PLOS ONE.* **12** (2), e0170597 (2017).
22 Jeffrey, N. S., Stephenson, R. S., Gallagher, J. A., Cox, P. Micro-computed tomography with iodine staining resolves the arrangement of muscle fibres. *Journal of Biomechanics.* **44**, 189-192 (2011).
23 Johnson, J. T. et al. Virtual Histology of Transgenic Mouse Embryos for High-Throughput Phenotyping. *PLOS Genetics.* **2**, e61 (2006).
24 Leszczyński, B. et al. Visualization and Quantitative 3D Analysis of Intraocular Melanoma and Its Vascularization in a Hamster Eye. *International Journal of Molecular Sciences.* **19** (2), 332 (2018).

25 Mizutani, R., Suzuki, Y. X-ray microtomography in biology. *Micron.* **43**, 104-115 (2012).
26 Busse, M. et al. Three-dimensional virtual histology enabled through cytoplasm-specific X-ray stain for microscopic and nanoscopic computed tomography. *Proceedings of the National Academy of Sciences of the United States of America.* **115** (10), 2293-2298 (2018).
27 Müller, M. et al. Non-destructive high-resolution 3D virtual histology enabled through a cell nucleus-specific stain for X-ray computed tomography. *Scientific Reports.* **8**, 17855 (2018).
28 Germany, Z. *ZEISS product information: ZEISS Xradia 510 Versa* <https://www.zeiss.com/microscopy/int/products/x-ray-microscopy/zeiss-xradia-510-versa.html> (April 10, 2019).
29 Nachtrab, F. et al. Development of a Timepix based detector for the NanoXCT project. *Journal of Instrumentation.* **10** (11), C11009 (2015).
30 Kraft, P. et al. Performance of single-photon-counting PILATUS detector modules. *Journal of Synchrotron Radiation.* **16** (3), 368-375 (2009).
31 Kraft, P. et al. Characterization and calibration of PILATUS detectors. *IEEE Transactions on Nuclear Science.* **56** (3), 758-764 (2009).
32 Germany, Z. *ZEISS product information: ZEISS Xradia 810 Ultra* <https://www.zeiss.com/microscopy/int/products/x-ray-microscopy/xradia-810-ultra.html> (April 9 2019).
33 Anderson, T. F. Techniques for the preservation of three-dimensional structure in preparing specimens for the electron microscope. *Transactions of the New York Academy of Sciences.* **13** (4 Series II), 130-134 (1951).
34 Bray, D. in *Supercritical Fluid Methods and Protocols. Methods in Biotechnology.* Vol. 13 eds J. R. Williams, A. A. Clifford) 235-243 (Humana Press, 2000).
35 Lucy, L. B. An iterative technique for the rectification of observed distributions. *The Astronomical Journal.* **79**, 745-765 (1974).
36 Richardson, W. H. Bayesian-Based Iterative Method of Image Restoration. *The Journal of the Optical Society of America.* **62** (1), 55-59 (1972).
37 Paganin, F., Mayo, S. C., Gureyev, T. E., Miller, P. R., Wilkins, S. W. Simultaneous phase and amplitude extraction from a single defocused image of a homogeneous object. *Journal of Microscopy.* **206**, 33-40 (2002).
38 Riedelsheimer, B., Büchl-Zimmermann, S. in *Mikroskopische Technik* 10.1007/978-3-642-55190-1 eds M. Mulisch & U. Welsch) Ch. 10, 193-194 (Spektrum-Verlag GmbH Berlin Heidelberg, 2015).
39 Hubbell, J. H., Seltzer, S. M. Tables of Xray mass attenuation coefficients and mass energy-absorption coefficients from 1 keV to 92 keV and 48 additional substances of dosimetric interest, Table 3. National Institute of Standards and Technology. NISTIR 5632 (1995).
40 Hong, H. Y., Yoo, G. S., Choi, J. K. An Eosin Y Method for Protein Determination in Solution. *Analytical Letters.* **32** (12), 2427-2442 (1999).
41 Bruker. *Bruker product information: SkyScan 2211*, <http://bruker-microct.com/products/2211.htm> (April 10, 2019).
42 Company, G. E. *GE product information: Phoenix nanotom m*, <https://www.gemeasurement.com/sites/gemc.dev/files/geit-31344en_nanotom_m_0517.pdf> (April 10, 2019).
43 Dierick, M. et al. Recent Micro-CT Scanner Developments at UGCT. *Nuclear Instruments*

573 *and Methods in Physics Research Section B.* **324**, 35-40 (2014).
574 44 Kastner, J., Plank, B., Heinzl, C. Advanced X‐ray computed tomography methods: High
575 resolution CT, quantitative CT, 4DCT and phase contrast CT in *Proceedings of Digital Industrial*
576 *Radiology and Computed Tomography.* 120-132 (2015).
577

Figure

Figure 1


Click here to access/download
Video or Animated Figure
JoVE_Figure 1.svg

Figure 2


Click here to access/download
Video or Animated Figure
JoVE_Figure 2.svg

Figure 3

Click here to access/download

Video or Animated Figure

JoVE_Figure 3.svg

Figure 4


Click here to access/download
Video or Animated Figure
JoVE_Figure 4.svg

Name of Material/ Equipment	Company
50 mL centrifuge tube by Falcon	VWR
Avizo Fire 8.1	Thermo Fisher Scientific
Bal-Tec CPD 030	Bal-Tec AG
Carbon dioxide cylinder with standpipe	Linde
Cellulose tissue paper	VWR
Desiccator by Duran	VWR
Disposable safety scalpel by Aesculap	VWR
Eosin Y disodium salt	Sigma-Aldrich
Ethanol absolute by Baker Analyzed	VWR
Forceps, by USBECK Laborgeräte	VWR
Formaldehyde solution, 37%	Carl Roth
Glacial acetic acid	Alfa Aesar
Microcentrifuge tubes by Eppendorf	VWR
nanofocus X-ray source as part of the nanoCT scanner	Excillum
Petri dish by Sterilin	VWR
Phosphate Buffered Saline (PBS)	Merck
PILATUS detector as part of the nanoCT scanner	Dectris
Plastic pasteur pipette	Carl Roth
Rocking Shaker ST5	CAT
Sample Tubes by Nalgene	Carl Roth
Silicone grease by Bayer	Sigma-Aldrich
Zeiss Xradia Versa 500	Zeiss

(1) Germany, Z. ZEISS product information: ZEISS Xradia 510 Versa <https://w
(2) Nachtrab, F. *et al.* Development of a Timepix based detector for the Nanc
(3) Kraft, P. *et al.* Performance of single-photon-counting PILATUS detector r
(4) Kraft, P. et al. Characterization and calibration of PILATUS detectors. IEEE
(5) Germany, Z. ZEISS product information: ZEISS Xradia 810 Ultra <https://w
(6) Company, G. E. GE product information: Phoenix nanotom m, <https://ww

Catalog Number	Comments/Description
734-0453	
	CO_2 as drying agent
3700113 115-0600 SCOT247826954	10 kg, short
AESCBA210 E4382	certified by Biological Stain Commission
80252500	
232-0096 CP10.2 36289.AP	acid-free, stabilized with ~10% MeOH
211-2120	safe-lock, 2.0 ml
391-2019	high-flux nanofocus X-ray transmission tube[2]; there are commercial
L1825	Dulbecco's formualtion, w/o calcium and magnesium
EA68.1 60281-0000 ATK5.1 85404	single-photon counting detector[3,4]; there are commercially availble graduated, 1 ml high-vacuum this microCT scanner has been updated[1]

/ww.zeiss.com/microscopy/int/products/x-ray-microscopy/zeiss-xradia-510-versa.html> (April 10, 2
oXCT project. *Journal of Instrumentation* **10** (11), C11009, (2015).
nodules. *Journal of Synchrotron Radiation* **16** (3), 368-375, (2009).
Transactions on Nuclear Science 56 (3), 758-764, (2009).
ww.zeiss.com/microscopy/int/products/x-ray-microscopy/xradia-810-ultra.html> (April 9 2019).
ww.gemeasurement.com/sites/gemc.dev/files/geit-31344en_nanotom_m_0517.pdf> (April 10, 201

lly availble nanoCT systems available[5,6]

nanoCT systems available [5,6]

2019).

.9).

jove 1 Alewife Center #200 Cambridge, MA 02140 tel. 617.945.9051 www.jove.com

ARTICLE AND VIDEO LICENSE AGREEMENT

Title of Article: 3D imaging of soft-tissue samples using an X-ray Spectral Staining method and nanoscopic Computed Tomography

Author(s): Madleen Busse, Mark Müller, Nelakurthi A. Kishan, Simone Hook, Sebastian Allner, Klaus Achterhold, Julia Herzen, Franz Pfeiffer

Item 1: The Author elects to have the Materials be made available (as described at http://www.jove.com/publish) via:

☐ Standard Access ☒ Open Access

Item 2: Please select one of the following items:

☒ The Author is **NOT** a United States government employee.

☐ The Author is a United States government employee and the Materials were prepared in the course of his or her duties as a United States government employee.

☐ The Author is a United States government employee but the Materials were NOT prepared in the course of his or her duties as a United States government employee.

ARTICLE AND VIDEO LICENSE AGREEMENT

1. **Defined Terms.** As used in this Article and Video License Agreement, the following terms shall have the following meanings: "**Agreement**" means this Article and Video License Agreement; "**Article**" means the article specified on the last page of this Agreement, including any associated materials such as texts, figures, tables, artwork, abstracts, or summaries contained therein; "**Author**" means the author who is a signatory to this Agreement; "**Collective Work**" means a work, such as a periodical issue, anthology or encyclopedia, in which the Materials in their entirety in unmodified form, along with a number of other contributions, constituting separate and independent works in themselves, are assembled into a collective whole; "**CRC License**" means the Creative Commons Attribution-Non Commercial-No Derivs 3.0 Unported Agreement, the terms and conditions of which can be found at: http://creativecommons.org/licenses/by-nc-nd/3.0/legalcode; "**Derivative Work**" means a work based upon the Materials or upon the Materials and other pre-existing works, such as a translation, musical arrangement, dramatization, fictionalization, motion picture version, sound recording, art reproduction, abridgment, condensation, or any other form in which the Materials may be recast, transformed, or adapted; "**Institution**" means the institution, listed on the last page of this Agreement, by which the Author was employed at the time of the creation of the Materials; "**JoVE**" means MyJove Corporation, a Massachusetts corporation and the publisher of The Journal of Visualized Experiments; "**Materials**" means the Article and / or the Video; "**Parties**" means the Author and JoVE; "**Video**" means any video(s) made by the Author, alone or in conjunction with any other parties, or by JoVE or its affiliates or agents, individually or in collaboration with the Author or any other parties, incorporating all or any portion of the Article, and in which the Author may or may not appear.

2. **Background.** The Author, who is the author of the Article, in order to ensure the dissemination and protection of the Article, desires to have the JoVE publish the Article and create and transmit videos based on the Article. In furtherance of such goals, the Parties desire to memorialize in this Agreement the respective rights of each Party in and to the Article and the Video.

3. **Grant of Rights in Article.** In consideration of JoVE agreeing to publish the Article, the Author hereby grants to JoVE, subject to **Sections 4** and **7** below, the exclusive, royalty-free, perpetual (for the full term of copyright in the Article, including any extensions thereto) license (a) to publish, reproduce, distribute, display and store the Article in all forms, formats and media whether now known or hereafter developed (including without limitation in print, digital and electronic form) throughout the world, (b) to translate the Article into other languages, create adaptations, summaries or extracts of the Article or other Derivative Works (including, without limitation, the Video) or Collective Works based on all or any portion of the Article and exercise all of the rights set forth in (a) above in such translations, adaptations, summaries, extracts, Derivative Works or Collective Works and(c) to license others to do any or all of the above. The foregoing rights may be exercised in all media and formats, whether now known or hereafter devised, and include the right to make such modifications as are technically necessary to exercise the rights in other media and formats. If the "Open Access" box has been checked in **Item 1** above, JoVE and the Author hereby grant to the public all such rights in the Article as provided in, but subject to all limitations and requirements set forth in, the CRC License.

4. **Retention of Rights in Article.** Notwithstanding the exclusive license granted to JoVE in **Section 3** above, the Author shall, with respect to the Article, retain the non-exclusive right to use all or part of the Article for the non-commercial purpose of giving lectures, presentations or teaching classes, and to post a copy of the Article on the Institution's website or the Author's personal website, in each case provided that a link to the Article on the JoVE website is provided and notice of JoVE's copyright in the Article is included. All non-copyright intellectual property rights in and to the Article, such as patent rights, shall remain with the Author.

5. **Grant of Rights in Video – Standard Access.** This **Section 5** applies if the "Standard Access" box has been checked in **Item 1** above or if no box has been checked in **Item 1** above. In consideration of JoVE agreeing to produce, display or otherwise assist with the Video, the Author hereby acknowledges and agrees that, Subject to **Section 7** below, JoVE is and shall be the sole and exclusive owner of all rights of any nature, including, without limitation, all copyrights, in and to the Video. To the extent that, by law, the Author is deemed, now or at any time in the future, to have any rights of any nature in or to the Video, the Author hereby disclaims all such rights and transfers all such rights to JoVE.

6. **Grant of Rights in Video – Open Access.** This **Section 6** applies only if the "Open Access" box has been checked in **Item 1** above. In consideration of JoVE agreeing to produce, display or otherwise assist with the Video, the Author hereby grants to JoVE, subject to **Section 7** below, the exclusive, royalty-free, perpetual (for the full term of copyright in the Article, including any extensions thereto) license (a) to publish, reproduce, distribute, display and store the Video in all forms, formats and media whether now known or hereafter developed (including without limitation in print, digital and electronic form) throughout the world, (b) to translate the Video into other languages, create adaptations, summaries or extracts of the Video or other Derivative Works or Collective Works based on all or any portion of the Video and exercise all of the rights set forth in (a) above in such translations, adaptations, summaries, extracts, Derivative Works or Collective Works and (c) to license others to do any or all of the above. The foregoing rights may be exercised in all media and formats, whether now known or hereafter devised, and include the right to make such modifications as are technically necessary to exercise the rights in other media and formats. For any Video to which this **Section 6** is applicable, JoVE and the Author hereby grant to the public all such rights in the Video as provided in, but subject to all limitations and requirements set forth in, the CRC License.

7. **Government Employees.** If the Author is a United States government employee and the Article was prepared in the course of his or her duties as a United States government employee, as indicated in **Item 2** above, and any of the licenses or grants granted by the Author hereunder exceed the scope of the 17 U.S.C. 403, then the rights granted hereunder shall be limited to the maximum rights permitted under such statute. In such case, all provisions contained herein that are not in conflict with such statute shall remain in full force and effect, and all provisions contained herein that do so conflict shall be deemed to be amended so as to provide to JoVE the maximum rights permissible within such statute.

8. **Protection of the Work.** The Author(s) authorize JoVE to take steps in the Author(s) name and on their behalf if JoVE believes some third party could be infringing or might infringe the copyright of either the Author's Article and/or Video.

9. **Likeness, Privacy, Personality.** The Author hereby grants JoVE the right to use the Author's name, voice, likeness, picture, photograph, image, biography and performance in any way, commercial or otherwise, in connection with the Materials and the sale, promotion and distribution thereof. The Author hereby waives any and all rights he or she may have, relating to his or her appearance in the Video or otherwise relating to the Materials, under all applicable privacy, likeness, personality or similar laws.

10. **Author Warranties.** The Author represents and warrants that the Article is original, that it has not been published, that the copyright interest is owned by the Author (or, if more than one author is listed at the beginning of this Agreement, by such authors collectively) and has not been assigned, licensed, or otherwise transferred to any other party. The Author represents and warrants that the author(s) listed at the top of this Agreement are the only authors of the Materials. If more than one author is listed at the top of this Agreement and if any such author has not entered into a separate Article and Video License Agreement with JoVE relating to the Materials, the Author represents and warrants that the Author has been authorized by each of the other such authors to execute this Agreement on his or her behalf and to bind him or her with respect to the terms of this Agreement as if each of them had been a party hereto as an Author. The Author warrants that the use, reproduction, distribution, public or private performance or display, and/or modification of all or any portion of the Materials does not and will not violate, infringe and/or misappropriate the patent, trademark, intellectual property or other rights of any third party. The Author represents and warrants that it has and will continue to comply with all government, institutional and other regulations, including, without limitation all institutional, laboratory, hospital, ethical, human and animal treatment, privacy, and all other rules, regulations, laws, procedures or guidelines, applicable to the Materials, and that all research involving human and animal subjects has been approved by the Author's relevant institutional review board.

11. **JoVE Discretion.** If the Author requests the assistance of JoVE in producing the Video in the Author's facility, the Author shall ensure that the presence of JoVE employees, agents or independent contractors is in accordance with the relevant regulations of the Author's institution. If more than one author is listed at the beginning of this Agreement, JoVE may, in its sole

jove

ARTICLE AND VIDEO LICENSE AGREEMENT

discretion, elect not take any action with respect to the Article until such time as it has received complete, executed Article and Video License Agreements from each such author. JoVE reserves the right, in its absolute and sole discretion and without giving any reason therefore, to accept or decline any work submitted to JoVE. JoVE and its employees, agents and independent contractors shall have full, unfettered access to the facilities of the Author or of the Author's institution as necessary to make the Video, whether actually published or not. JoVE has sole discretion as to the method of making and publishing the Materials, including, without limitation, to all decisions regarding editing, lighting, filming, timing of publication, if any, length, quality, content and the like.

12. **Indemnification.** The Author agrees to indemnify JoVE and/or its successors and assigns from and against any and all claims, costs, and expenses, including attorney's fees, arising out of any breach of any warranty or other representations contained herein. The Author further agrees to indemnify and hold harmless JoVE from and against any and all claims, costs, and expenses, including attorney's fees, resulting from the breach by the Author of any representation or warranty contained herein or from allegations or instances of violation of intellectual property rights, damage to the Author's or the Author's institution's facilities, fraud, libel, defamation, research, equipment, experiments, property damage, personal injury, violations of institutional, laboratory, hospital, ethical, human and animal treatment, privacy or other rules, regulations, laws, procedures or guidelines, liabilities and other losses or damages related in any way to the submission of work to JoVE, making of videos by JoVE, or publication in JoVE or elsewhere by JoVE. The Author shall be responsible for, and shall hold JoVE harmless from, damages caused by lack of sterilization, lack of cleanliness or by contamination due to the making of a video by JoVE its employees, agents or independent contractors. All sterilization, cleanliness or decontamination procedures shall be solely the responsibility of the Author and shall be undertaken at the Author's expense. All indemnifications provided herein shall include JoVE's attorney's fees and costs related to said losses or damages. Such indemnification and holding harmless shall include such losses or damages incurred by, or in connection with, acts or omissions of JoVE, its employees, agents or independent contractors.

13. **Fees.** To cover the cost incurred for publication, JoVE must receive payment before production and publication of the Materials. Payment is due in 21 days of invoice. Should the Materials not be published due to an editorial or production decision, these funds will be returned to the Author. Withdrawal by the Author of any submitted Materials after final peer review approval will result in a US$1,200 fee to cover pre-production expenses incurred by JoVE. If payment is not received by the completion of filming, production and publication of the Materials will be suspended until payment is received.

14. **Transfer, Governing Law.** This Agreement may be assigned by JoVE and shall inure to the benefits of any of JoVE's successors and assignees. This Agreement shall be governed and construed by the internal laws of the Commonwealth of Massachusetts without giving effect to any conflict of law provision thereunder. This Agreement may be executed in counterparts, each of which shall be deemed an original, but all of which together shall be deemed to me one and the same agreement. A signed copy of this Agreement delivered by facsimile, e-mail or other means of electronic transmission shall be deemed to have the same legal effect as delivery of an original signed copy of this Agreement.

A signed copy of this document must be sent with all new submissions. Only one Agreement is required per submission.

CORRESPONDING AUTHOR

Name:	Dr. Madleen Busse
Department:	Department of Physics & Munich School of BioEngineering
Institution:	Technical University of Munich
Title:	Dr. (PhD)
Signature:	
Date:	12.05.2019

Please submit a **signed** and **dated** copy of this license by one of the following three methods:

1. Upload an electronic version on the JoVE submission site
2. Fax the document to +1.866.381.2236
3. Mail the document to JoVE / Attn: JoVE Editorial / 1 Alewife Center #200 / Cambridge, MA 02140

Technical University of Munich | Chair of Biomedical Physics
Boltzmannstraße 11 | 85748 Garching

BY ELECTRONIC SUBMISSION
JoVE

Garching, 14th June 2019

RE: Manuscript revision "3D imaging of soft-tissue samples using an X-ray specific staining method and nanoscopic computed tomography" by Madleen Busse and co-authors

Dear Review Editor, Phillip Steindel,

Thank you for accommodating an efficient review of our manuscript. We were pleased to read the general positive responses of the reviewers and thank them for their constructive comments.
Please find below our point-by-point response to the reviewers' comments (in bold). We have modified the manuscript to clarify the addressed issues and included the reviewers' suggestions. We list these modifications, where appropriate, in the text below.
Please note that we submitted two revised version of the manuscript including line numbers as communicated via email.
The file '60251_R0_051419_MBusse' has the final reference list included, and therefore, no track changes are present. The file '60251_R0_051419_track changes_MBusse' does not have the final reference list but includes all the changes made to the manuscript as part of the review. We would like to kindly ask you to forward the revised file to the reviewers in conjunction with the point-by-point response, as we refer in our answers to line numbers in the manuscript (with respect to file '60251_R0_051419_MBusse').

We hope that our amendments fulfill yours and the reviewers' expectations and that you may now consider our manuscript suitable for publication in *JoVE*.

Sincerely yours,

Madleen Busse
(on behalf of all co-authors)

Technical University of Munich
Chair of Biomedical Physics,
Department of Physics and
Munich School of Bioengineering

Dr. Madleen Busse
Marie Skłodowska-Curie Fellow
Boltzmannstraße 11
85748 Garching

Tel. +49 89 289 10802
Fax +49 89 289 10805

madleen.busse@tum.de
www.e17.ph.tum.de
www.tum.de

POINT-BY-POINT RESPONSE

EDITOR'S REMARKS TO AUTHOR:

General:
1. Please take this opportunity to thoroughly proofread the manuscript to ensure that there are no spelling or grammar issues.

We have taken the opportunity to thoroughly proofread the manuscript and have edited the following spelling and grammar issues:

page 3, line 98: 'histopathlogical' has been changed to 'histopathological' and 'charcaterization' has been changed to 'characterization'

page 3, line 121: 'Centrifuge Tube' has been to 'centrifuge tube'

page 3, line 132: 'Centrifuge Tube' has been to 'centrifuge tube'

page 4, line 133: 'Centrifuge Tube' has been to 'centrifuge tube'

page 10, line 397: 'an result' has been changed to 'a result'

2. Please revise lines 187-192, 207-211, 273-279, 293-296, and 263-268 to avoid previously published text.

We thank the editor for outlining text that is closely related to the previously published text. We assume that the editor meant lines 363-368 instead of 263-268. Please find below the changes made to the manuscript.

page 5, lines 187-192: The paragraph 'Note: The overview CT data were acquired with the 0.39x camera objective and an exposure time of 2 s per projection with an effective pixel size of 12 µm. This overview CT data were used to identify the ROI for the high-resolution CT scan, which was selected using the integrated scout and scan software tool of the ZEISS Xradia 500 Versa. The high-resolution CT data were acquired with the 4x objective and an exposure time of 15 s per projection with an effective pixel size of 3.3 µm.' has been rewritten to avoid previously published text. At the same time, the commercial language has been removed from the text (see comment 3 from the editor below). Please find below the rewritten paragraph (page 5, lines 190-197):

'Note: The acquisition parameters for the overview CT scan were chosen for best image quality. As such the 0.39x camera objective was chosen to cover the whole

sample within the field of view (FOV). This resulted in an effective pixel size of 12 µm. The exposure time of 2 s per projection provided a good signal to noise ratio. The ROI for the high-resolution CT scan was identified using the microCT data from the overview scan. MicroCT scanners often incorporate an integrated software tool, which allows for the precise selection of the determined ROI. For the high-resolution CT data, the 4x camera objective was chosen resulting in an effective pixel size of 3.3 µm. Here, an exposure time of 15 s per projection was needed.'

page 5, lines 207-211: The following text 'Note: The X-ray nanoCT measurements were performed with an in-house developed nanoCT system that consists of a novel nanofocus X-ray source (prototype nanotube, Excillum, Sweden)[23] and a single-photon counting detector (PILATUS 300K-W 20 Hz, Dectris, Switzerland)[24,25]. The lens-free device is based on mere geometrical magnification and can generate 3D data with resolutions down to 100 nm[10]. However, nanoCT systems are commercially available such as the Xradia Ultra 810 from Zeiss[26].' has been rewritten. At the same time, the commercial language has been removed from the text (see comment 3 from the editor below). The citations associated with maerials used for the experiment have been removed from the reference list and are now linked to the Table of Materials. Please find below the rewritten paragraph (page 5, lines 212-215):

'Note: The X-ray nanoCT scanner has been developed in-house. The lens-free instrument is equipped with a nanofocus X-ray source and a single-photon counting detector. 3D data with resolutions down to 100 nm can be generated[10]. Generally, nanoCT systems including those with X-ray optics are commercially available and not limited to the described nanoCT scanner.'

page 7, lines 273-279: The paragraph 'Note: For this voxel size, the field of view (FOV) of a single CT measurement is given by approximately 560 µm in the direction perpendicular to the rotation axis (horizontal) and 75 µm in the direction of the rotation axis (vertical). However, the FOV can be extended along the rotation axis by combining multiple scans at different vertical positions to a larger volume. Furthermore, the possibility of local tomography measurements allows for larger sample diameters perpendicular to the rotation axis than given by the FOV of a global CT measurement. The exposure time per image was 4 s resulting in a total acquisition time per data set of approximately 3.5 h.' has been rewritten to avoid previously published text. Please find below the rewritten paragraph (page 7, lines 289-296):

‘Note: A single CT measurement acquired at 400 nm voxel size has a FOV of 75 µm in the direction of the rotation axis (vertical) and approximately 560 µm in the direction perpendicular to the rotation axis (horizontal). To investigate larger volumes, an extension of the FOV along the rotation axis can be achieved by combining multiple scans at different vertical positions. Additionally, local tomography scans can be performed to measure samples with a larger sample diameter perpendicular to the rotation axis than given by the FOV of a global CT scan. The nanoCT data was acquired with an exposure time of 4 s per projection. As such the total acquisition time per data set was approximately 3.5 h.’

page 7, lines 293-296: The following text ‘Note: The minimum intensity projection slices shown in Figure 3 were generated by calculating the minimum value for each pixel in 18 adjacent slices, which corresponds to a virtual slice thickness of approximately 7µm. The volume rendering of the nanoCT data shown in Figure 4 were generated with Avizo Fire 8.1 (Thermo Fisher Scientific).’ has been altered. At the same time, the commercial language has been removed from the text (see comment 3 from the editor below). Please find below the rewritten paragraph (page 8, lines 309-313):

‘Note: Figure 3 evaluates the obtained nanoCT data with corresponding histological sections, which were approximately 7µm thick. Therefore, minimum intensity projection slices of 18 adjacent nanoCT slices with a virtual thickness of approximately 7µm were generated by means of calculating the minimum value for each pixel in the relevant slices. A visualization software was used to render the volume of the nanoCT data, which is displayed in Figure 4.’

page 9, lines 363-368: The following text ‘Here, the aspect of the low intrinsic attenuation properties of soft tissue for typically used X-ray energies of laboratory-based microCT systems, which consists of mainly carbon, hydrogen, oxygen and nitrogen[31] and the low concentration of eosin used for staining were seen as the limiting factor. The sensitivity levels required for X-ray CT imaging were not met with regards to the high atomic number element bromine (Z = 35)[31], of which one eosin molecule holds four bromide atoms being covalently bound to the fluorescein core.’ has been rewritten to avoid previously published text. Please find below the rewritten paragraph (page 9, lines 380-386):

‘On the one hand, this can be attributed to the low intrinsic attenuation properties of soft tissue for typically used X-ray energies of laboratory-based microCT systems. Usually, soft tissue is composed of mainly carbon, hydrogen, oxygen and nitrogen[34], and therefore, does not result in contrast enhancement. On the other

hand, the low concentration of eosin used for staining was the limiting factor. Even though one eosin molecule holds four bromide atoms (high atomic number element bromine with Z = 35[34]), the sensitivity levels required for X-ray CT imaging were not met.'

3. JoVE cannot publish manuscripts containing commercial language. This includes trademark symbols (™), registered symbols (®), and company names before an instrument or reagent. Please limit the use of commercial language from your manuscript and use generic terms instead. All commercial products should be sufficiently referenced in the Table of Materials and Reagents. For example: Eppendorf, Zeiss, Pilatus, etc.

page 4, line 152: 'an Eppendorf Tube' has been deleted and the new term 'a conical sample container' was inserted

page 4, line 155: 'an Eppendorf Tube' has been deleted and the new term 'a conical sample container' was inserted

page 4, line 160: 'an Xradia 500 Versa from Zeiss' has been deleted and the new term 'a microCT scanner' was inserted

page 4, lines 163 and 164: The entire sentence 'The microCT scanner is commercially available[22].' has been deleted from the manuscript to remove commercial language. Therefore, also reference 22 (Germany, Z. *ZEISS product information: ZEISS Xradia 510 Versa* <https://www.zeiss.com/microscopy/int/products/x-ray-microscopy/zeiss-xradia-510-versa.html> (April 10, 2019).) has been deleted from the manuscript. This reference has been added to the Table of Materials.

page 5, lines 193-195: The sentence 'This overview CT data were used to identify the ROI for the high-resolution CT scan, which was selected using the integrated scout and scan software tool of the ZEISS Xradia 500 Versa.' has been rewritten to avoid commercial language. The changes are 'The ROI for the high-resolution CT scan was identified using the microCT data from the overview scan. MicroCT scanners often incorporate an integrated software tool, which allows for the precise selection of the determined ROI.'

page 5, lines 205-206: The sentence 'The volume renderings of the microCT data shown in Figure 1 and 2 were generated with Avizo Fire 8.1 (Thermo Fisher Scientific).' has been altered to 'The volume renderings of the microCT data shown in Figure 1 and 2 were generated using a visualization software.'

page 5, lines 212-215: The following paragraph contained several commercial language phrases, which were all deleted. The rewritten paragraph reads as follows: 'Note: The X-ray nanoCT scanner has been developed in-house. The lens-free instrument is equipped with a nanofocus X-ray source and a single-photon counting detector. 3D data with resolutions down to 100 nm can be generated[10]. Generally, nanoCT systems including those with X-ray optics are commercially available and not limited to the described nanoCT scanner.' The references 23-25 have been deleted from the manuscript as they hold commercial language in the title. These references have been added to the Table of Materials.

page 6, lines 237-238: The following sentence was deleted to remove commercial language from the manuscript 'In case of the mouse kidney VOIs, a Bal-TEC CPD 030 with CO_2 as drying agent was used.'

page 8, lines 313-314: The sentence 'The volume rendering of the nanoCT data shown in Figure 4 were generated with Avizo Fire 8.1 (Thermo Fisher Scientific).' has been rewritten to 'A visualization software was used to render the volume of the nanoCT data, which is displayed in Figure 4.'

page 8, line 336: To avoid commercial language, the sentence 'Both data sets were acquired with the Xradia Versa 500 microCT using identical acquisition parameters.' has been changed to 'Both microCT data sets were acquired using identical acquisition parameters.'

Protocol:
1. For each protocol step/substep, please ensure you answer the "how" question, i.e., how is the step performed? Alternatively, add references to published material specifying how to perform the protocol action. If revisions cause a step to have more than 2-3 actions and 4 sentences per step, please split into separate steps or substeps.

Specific Protocol steps:

1. 3.4: This step is fairly vague; please either include specific computational steps or do not highlight.

To our understanding, the specific protocol step 3.4 contains already a very detailed description on the individual steps undertaken to process the data set. Including the individual computational instructions for each step by means of introducing the computational code used, would go beyond the scope of this manuscript. It should be noted that each acquired data set has its own challenges with respect to data processing, which can be addressed in different ways

depending on the reconstruction software and image processing tools used. Therefore, we have chosen to not highlight this section.

Figures:
1. Please obtain explicit copyright permission to reuse any figures from a previous publication. Explicit permission can be expressed in the fo rm of a letter from the editor or a link to the editorial policy that allows re-prints. Please upload this information as a .doc or .docx file to your Editorial Manager account.

The authors have gained permission from PNAS to reuse the material from the figures of the previous publication. The communication was done via email exchange. To upload a .docx file, the content of the email was copied into Word. The requested document has been uploaded to the Editorial Manager account. The original email can be forwarded to the editor upon request.

Discussion:
1. Discussion: As we are a methods journal, please revise the Discussion to explicitly cover the following in detail in 3–6 paragraphs with citations:
a) Critical steps within the protocol
b) Any modifications and troubleshooting of the technique
c) Any limitations of the technique

The discussion consists of 6 paragraphs, which focus all on the described method addressing to the authors understanding the desired points mentioned above. However, the authors have added some additional information to outline some further limitations of the technique. The changes to the manuscript are listed below:

page 10, line 407-414: 'It should be noted that the overall staining time and volume of the staining solution needed might request some adaptations depending on the nature of the sample. Nevertheless, the eosin-based staining protocol is suitable for whole-organ staining, which then enables high resolution microCT imaging of whole organs. Shrinkage artifacts due to the solvent ethanol, which was used to keep the sample moist during the microCT measurements, were not observed. Additional preparation steps are required for nanoCT imaging, which allows for the investigation of smaller tissue pieces retrieved from the original sample.'

page 10, line 407-414: 'The application of histological counter staining is currently limited to the H-stain. Other standard histological counter stainings such as periodic acid Schiff's base, Elastica van Gieson or Gomorri silver have to be evaluated as well as the compatibility with immunohistological techniques needs to be tested.'

References:
1. Please do not abbreviate journal titles.

The authors have added the full journal titles to all entries where appropriate under references instead of using abbreviated journal titles. Since the references are linked directly to a reference management software, the individual changes had to be incorporated directly into the manuscript. The individual changes have not been listed here.

2. Please do not include product manuals in the references; these can be linked to in the Table of Materials.

The references 22-26 as well as 33 and 34, which are linked to a product were deleted from the manuscript. They are now linked to the Table of Materials where appropriate.

Table of Materials:
1. Please ensure the Table of Materials has information on all materials and equipment used, especially those mentioned in the Protocol.

The authors added the mentioned detector and X-ray source as part of the nanoCT scanner to the Table of Materials and deleted the direct product link from the manuscript (see section 2 and 3 under general remarks above). The references, which are cited when stating these devices, have been added where appropriate, as well as some links to other nanoCT scanners, which are commercially available.

2. Please remove trademark (™) and registered (®) symbols from the Table and Materials.

All trademark (™) **and registered** (®) **symbols have been removed from the Table of Materials.**

A revised Table of Materials (JoVE_Materials_revised_MBusse_2019) has been uploaded as part of the revised submission.

REVIEWER #1 (COMMENTS):

Manuscript Summary:

I welcome the idea to implement the presented workflow by Madleen Busse and co-authors as a JoVE video tutorial. I already read the original 2018 PNAS paper "Three-dimensional virtual histology enabled through cytoplasm-specific X-ray stain for microscopic and nanoscopic computed tomography" with high interest and I am convinced that the presented workflow is of broad interest for the biological imaging community.

The presented paper is the detailed technical workflow description for the 2018 PNAS paper. As such, there are many redundancies to the PNAS paper including most of the figures, but also some novel and more detailed information on the technical workflow. As stated in the "Criteria for Publication" on the JoVE webpage this is in line with the scope of the journal. I don´t know about the copyright issues with previously published figures, but as the JoVE webpage states "We do not republish data or results without the express permission of the original publisher" I will not comment on this issue, as I take for granted that the two publishers resolve any copyright issues and conflicts of interest.

The authors have gained permission from PNAS to reuse the figure material from the original article. A written statement from the PNAS editorial office has been submitted as part of the revision process.

The language and presentation style is generally good, and the presented protocol is detailed enough to make it fully reproducible. I thus look forward to see this paper as a video presentation. I have no major criticism to address, just a couple of suggestions for minor/discretionary revisions:

We thank reviewer 1 for the overall positive response. We have addressed all the comments expressed by reviewer 1 and hope that the reviewer finds our manuscript now suitable for publication in JoVE.

Page 3, Line 80: Rephrase "X-ray active", by for example "X-ray dense" or "radiodense", to me "X-ray active" is misleading as it could be mistaken as "emitting X-rays"

page 2, line 80: The wording ‘X-ray active contrast agent’ has been rephrased to ‘staining agents, which enhance the X-ray attenuation contrast.’ With reference to ‘X-ray active’ the authors have removed active from the sentence on page 2, line 87 to avoid confusing.

Page 4, Line 82: References 14-19: In my opinion this is not the best set of references

concerning contrast-enhancement for microCT imaging. Some rather important papers are missing here (like the Mizutani and Suzuki 2012 paper, "X-ray microtomography in biology", or the Johnson et al. 2006 paper "Virtual histology of transgenic mouse embryos for high-throughput phenotyping"), while some of the listed papers (e.g. Pauwels et al) are very exploratory without performing systematic tests or providing substantial (=useful!) data to characterize the tested stains.

We acknowledge the reviewer's comment to expand the introduction with regards to contrast enhancement for microCT imaging. The authors have extended the manuscript within the introduction section accordingly (page 2, line 82) and have added the suggested references by the reviewer to the reference list. Those together with additional references are listed below showing the reference number the reference has in the revised manuscript:

(20) Degenhardt, K., Wright, A. C., Horng, D., Padmanabhan, A. & Epstein, J. A. Rapid 3D phenotyping of cardiovascular development in mouse embryos by micro-CT with iodine staining. *Circulation: Cardiovascular Imaging.* 3 (3), 314-322, (2010).

(21) Dullin, C. *et al.* µCT of ex-vivo stained mouse hearts and embryos enables a precise match between 3D virtual histology, classical histology and immunochemistry. *PLOS ONE.* 12 (2), e0170597, (2017).

(22) Jeffrey, N. S., Stephenson, R. S., Gallagher, J. A. & Cox, P. Micro-computed tomography with iodine staining resolves the arrangement of muscle fibres. *Journal of Biomechanics.* 44 189-192, (2011).

(23) Johnson, J. T. *et al.* Virtual Histology of Transgenic Mouse Embryos for High-Throughput Phenotyping. *PLOS Genetics.* 2 e61, (2006).

(24) Leszczyński, B. *et al.* Visualization and Quantitative 3D Analysis of Intraocular Melanoma and Its Vascularization in a Hamster Eye. *International Journal of Molecular Sciences.* 19 (2), 332, (2018).

(25) Mizutani, R. & Suzuki, Y. X-ray microtomography in biology. *Mircon.* 43 104-115, (2012).

This publication provides by no means a complete library on all work that has been done within this field of research. Therefore, only a small selection of some research papers can be presented. We hope that the expanded list of references is representing now better the diversity of the field.

Page 4, Line 121: It would be very interesting to know the exact pH of the fixative as the authors mention that acidic fixation is critical.

The authors thank the reviewer for the interest in the pH value. The fixative solution without acetic acid has a neutral pH of 7, whereas the acidified fixative solution has a pH value of approximately 3. The authors have included that detail to the note of

the specific protocol step 1.1 on page 3, lines 126-127 ‘During acidification the pH of the fixative solution is changing from neutral to approximately 3.’

Page 5, Line 178: I am not sure whether "anchorage" is the correct term here. Maybe consider rephrasing by "the sample is wrapped in cellulose paper soaked with 70% ethanol…"

We thank the reviewer for the critical view and acknowledge the helpful suggestion. The sentence ‘If the sample holder does not allow to hold solvent at the bottom, the anchorage of a cellulose paper soaked with 70% (v/v) ethanol is suitable.’ has been rewritten to ‘If the sample holder does not allow to hold solvent at the bottom, a cellulose paper moistened with 70% (v/v) ethanol can be placed in the sample holder.’ and is now at page 5, lines 180-181 in the manuscript.

Page 6, Line 211: Maybe rephrase " nanoCT Systems" by "nanoCT systems including X-ray optics"

page 5, line 214-215: The sentence ‘However, nanoCT systems are commercially available such as the Xradia Ultra 810 from Zeiss[26].’ has been altered to ‘Generally, nanoCT systems including those with X-ray optics are commercially available and not limited to the described nanoCT scanner.’

Page 6, Line 217: Maybe rephrase "reflecting-light microscope" by "stereomicroscope"

page 6, line 220: The wording ‘reflecting-light microscope’ has been rephrased to ‘stereomicroscope’.

Page 9, Line 319: It would be very interesting at this point to get some quantitative information on staining intensity and contrast (intensity values of stained tissue either in HU or linear attenuation μ). This would allow comparing staining intensity to other contrast agents such as Lugols, PTA, or OsO4.

The authors acknowledge the reviewer’s suggestion and the ability to provide quantitative information with respect to staining intensity and contrast, which would be indeed very beneficial. However, this challenge is not that easily solved. Even though the acquisition parameters might be identical for each measurement, the X-ray flux differs (quite often even during one measurement, whereby multiple flat field projections during one measurement can address this issue). Therefore, a calibration holding different concentrations of the staining solution becomes necessary for each measurement. The implementation of a calibration can be challenging with respect to space for the sample holder and the available FOV. A second aspect concerns the reliable and reproducible preparation of the

calibration solutions, especially if no standards are commercially available. As a last aspect, it should be mentioned that it would be rather a range of intensity values for different tissue types, as biological samples (even though they might be the same type) differ e.g. in size, shape and appearance. On a molecular level this could mean that one kidney holds more cytoplasm proteins and peptides compared to a second kidney sample (in case of the eosin stain). To gain a statistical significance, a lot of tissue samples must be measured to get to know that range of intensity values. Thus, getting quantitative information with respect to staining intensity and contrast has to be addressed in further studies.

Page 10, Line 360: Remove "2D", as slices have a certain thickness of several microns an thus are also 3D.

page 9, line 378: We acknowledge the reviewer's concern raising from the statement. Thus, we have removed '2D' from the text.

Page 19: I don´t understand those text fragments?

The authors do not understand this comment by the reviewer. The commented manuscript has 12 pages, and therefore, page 19 does not exist. The authors checked the manuscript carefully for 'text fragments' but could not find any.

REVIEWER #2 (COMMENTS):

Manuscript Summary:

The manuscript presents a protocol for staining of a fixed sample in brominated eosin in preparation for micro-CT and nano-CT imaging on commercial sources, and shows data from both. This type of work is important to this nascent field, and therefore would best be done in a way that will draw in users and demonstrate the technique's value. Their presented figures, both new and adapted from their 2018 paper, show the typical output of their full image acquisition pipeline with a comparison in resolution to classical histology. This protocol lowers the barrier to entry for labs interested in sample staining for soft-tissue micro/nano-CT and 3D histology at large, while familiarizing new potential users with the technology and its capabilities. The inclusion of imaging parameters, including detailed information on the field of view and resolution of acquired projections, particularly helps in this endeavor. The steps laid out for staining with eosin, micro-CT image acquisition, and nano-CT image acquisition are both straightforward and easy to follow in their written form, but areas regarding custom sample holders and staining prep will inevitably be made even clearer with the generation of the video protocol. However, the protocol's sole focus on cytoplasmic staining, as well as the presentation of some of the figures limits the power of this method for relating directly to histopathology.

We thank reviewer 2 for the suggestions made and the points of concerns raised. We have addressed all the comments expressed by reviewer 2 and hope that the reviewer finds our manuscript now suitable for publication in JoVE.

Major Concerns:

In the development of this new application of CT to the histological interpretation of 3D images, it is valuable to see what can be done with cytoplasmic staining. However, due to the proposed utility of the method in histopathological analysis, it is critical to show both nuclear and cytoplasmic staining. In lieu of a secondary nuclear stain, it might be more informative to label this protocol as a step towards full histopathological analysis and not a complete accomplishment of it. In addition, the authors' choice to use minimum intensity projections over a 7 micron thickness for visualizing their nano-CT data in comparison to histology needs to be better explained. Additionally, it is important to show the advantages of nano-CT namely higher resolution, which would benefit from the showing of single slice results and its limitations.

The authors thank the reviewer for the critical statement, which puts emphasis on 'cytoplasmic staining only', which has been exactly what the authors tried to implement, since an X-ray suitable staining agent, which enhances the attenuation contrast by specifically targeting the cytoplasm has not been described so far. Thus, a first step towards a multiple staining approach is the development of individual staining agents and/or staining procedures. In a second step, these

individual staining methods might be joined to allow for simultaneous visualization of different cellular compartments. Furthermore, staining a large *ex vivo* biological sample (such as a whole organ) is quite challenging compared to a few micrometers thick histological section.

The authors have nowhere in their manuscript stated that the described method is able to do 'a full histopathological analysis' nor that it is a 'complete accomplishment of it'. We have also not intended to reflect that view. The authors rather see 3D X-ray histology as a tool, which will support the pathologist as it will allow to non-destructively investigate the provided sample in 3D prior to further histopathological investigations. This can be e.g. read in the long abstract of the manuscript on page 2, lines 45-48 'Thereby, soft-tissue morphology with a similar detail level as the corresponding histological light microscopy images is reproduced. Deeper insights into the 3D configuration of tissue structures are achieved without impeding further investigations through histological methods.' Here, the authors emphasize that additional histopathological investigations are possible. The authors state this also as 'full compatibility with histopathology' (e.g. page 2, line 85), which is not be confused with 'full histopathological analysis' or 'complete accomplishment of it'.

The second aspect concerns the minimum intensity projections. The reviewer most likely refers to page 9, lines 357-359 '(b) Minimum intensity projection slice derived from the same nanoCT data set shown in (a) with a virtual slice thickness of approximately 7 µm, which allows for clear visualization of the cell nuclei.' being part of the figure caption related to Figure 3. Panel (a) of Figure 3 shows one individual nanoCT slice, which is approximately 400 nm thick. The individual slice thickness of one nanoCT slice is explicitly stated on page 9, lines 367-370 'The nanoCT image … with a voxel size of approximately 400nm.' Thus, individual nanoCT slices are shown within the manuscript. A more detailed explanation on how and why the virtual slice thickness of approximately 7 µm was processed is given in the protocol's note on page 8, lines 310-313 'Figure 3 evaluates the obtained nanoCT data with corresponding histological sections, which were approximately 7 µm thick. Therefore, minimum intensity projection slices of 18 adjacent nanoCT slices with a virtual thickness of approximately 7µm were generated by means of calculating the minimum value for each pixel in the relevant slices.' The why has been added to the revised manuscript, which hopefully makes this aspect clearer. Furthermore, the discussion at page 10, lines 422-428 'The nanoCT slice with a virtual thickness of approximately 400 nm (Figure 3a) compares already very well with the histological section (Figure 3c), which was derived from the corresponding soft-tissue sample. Considering the approximate thickness of a histological section with 7-10 µm, the generation of minimum intensity projection slices of the nanoCT data (Figure 3b), which correspond to a virtual thickness of approximately 7µm, allows for a better comparison with the histological section

(Figure 3c).' is explaining the why again. With this, we hope to ease the reviewer's concern with respect to the minimum intensity projections.

The primary applications of the data shown are in the realm of histopathology. In short, the design of the protocol and more importantly the interpretation of resultant data would benefit from greater awareness of the basic needs of histopathological diagnostics, whose basics include the ability to see all cellular components at once – especially nuclei.

The authors thank the reviewer for the critical thoughts with respect to the primary application in histopathology. The authors have made quite some efforts to gain the pathologists interest and have developed a strong and mutual relationship with the department of pathology. As such the basic needs of histopathological diagnostics are known to the authors and we do think that our described staining method meets the requirements to allow histopathological diagnostics – especially in the comparative approach. The authors have not expressed their wish to solely use their method for histopathological diagnostics in the manuscript. We rather see 3D X-ray histology as a tool, which will support the pathologist as it will allow to non-destructively investigate the provided sample in 3D prior to further histopathological investigations.

After all, a histological stain quite often also targets only one specific cellular compartment and a second stain is needed to highlight another. It should be also noted that not every stain is compatible with each other. The classical standard H&E stain does also not visualize 'all cellular compartments at once' as they only highlight the nuclei and the cytoplasm. This is also achieved with the X-ray eosin stain, whereby the cell nuclei are indirectly highlighted. Thus, the histopathologist can navigate through the sample and will be able to identify volumes of interest that need to be investigated further in 2D using histopathological methods including immunohistological methods. At last, histology has surely a historical advantage as time and experience have mastered several valuable staining procedures, which still must evolve for computed tomography.

Additionally, a clearer definition of what is meant by non-destructive imaging would be appropriate. One of the greatest strengths of CT, in any of its forms, is the preservation of the original sample being imaged for easier overlay work with other imaging modalities or analysis tools. It would be beneficial to emphasize the need for cutting the sample in between performing the micro-CT and nano-CT pipelines as well as to elaborate on alternative mechanisms for long-term sample storage after initial image acquisition.

We acknowledge the reviewer's concern. The staining method itself is suitable to stain whole organs completely and homogenously, which is an issue for several contrast agents currently available for CT and also standard histology. During the microCT investigations the stained mouse kidney stayed intact. It is correct that

for the nanoCT investigations, which provide the highest resolutions and sub-cellular structural information, the whole organ had to be sectioned and CPD was applied. As suggested by the reviewer, we clarified this point by adding an additional sentence to the discussion (page 10, lines 409-414):

‘Nevertheless, the eosin-based staining protocol is suitable for whole-organ staining, which then enables high-resolution microCT imaging of whole organs. Shrinkage artifacts due to the solvent ethanol, which was used to keep the sample moist during the microCT measurements, were not observed. Additional preparation steps are required for nanoCT imaging, which allows for the investigation of smaller tissue pieces retrieved from the original sample.’

With reference to the long-term sample storage after initial image acquisition, the authors have not encountered any problems. Maybe the reviewer is thinking of the storage above ethanol, which is not the case for the long-term storage. Once the sample has been imaged at the microCT and the data is of the desired quality, most of the sample is forwarded to histopathology, where the sample is embedded into paraffin and processed accordingly. Any leftovers of the paraffin block allow for long-term storage. The remaining sample is CPD tried, and therefore, stored in a desiccator for long-term use. Here, only the drying agent needs to be renewed when necessary to keep the samples free from moisture.

To that extent an additional note has been added to the manuscript referring to the special protocol step 3.1.1 (page 6, lines 225-227):

‘Note: The other halve of the mouse kidney was transferred to histopathology, where the sample was embedded into paraffin and processed accordingly to yield the typical histological sections as seen in Figure 3c and d.’

The small fields of view of nano CT indicates that joining fields would be valuable. A more investigative study could quantitate the effect of sample size on resolution. The answer to this question affects the power of potentially focusing in on one area of a larger sample for nanoCT. To what extent is this possible?

The authors thank the reviewer for showing interest in scanning larger samples, which is to some extend possible. A detailed description can be found in the manuscript on page 7, lines 289-296 ‘Note: A single CT measurement acquired at 400nm voxel size has a FOV of 75µm in the direction of the rotation axis (vertical) and approximately 560µm in the direction perpendicular to the rotation axis (horizontal). To investigate larger volumes, an extension of the FOV along the rotation axis can be achieved by combining multiple scans at different vertical positions. Additionally, the FOV of a local tomography measurement compared to

a global CT measurement offers the advantage to measure samples with a larger sample diameter perpendicular to the rotation axis.' It should be noted that the effective resolution for a specific measurement is not only depending on the sample size but also on several other factors such as the scattering properties of the sample and the sample stability during the measurement. Therefore, a general quantitative statement about the resolution depending on the sample size cannot be provided. We hope that this explanation is satisfying and answers the reviewer's question.

Cell membranes clearly visible in the lumen of the tubules were not detectable using nano-CT, which should have adequate resolution for them to be represented. This might be an effect of contrast adjustment in the figure itself and would be beneficial to correct in the JOVE video.

We acknowledge the reviewer's statement with reference to the brush border. It is correct that these are not visible within the lumen of the tubules on the corresponding nanoCT slices. Evidence that the structures were present and stained show the corresponding histological sections (Figure 3c and d). The authors are aware of this and can ensure that contrast adjustment has been carefully checked. One explanation is seen in the rather low sensitivity level of CT, i.e. a certain amount of staining agent is needed to visualize structural details. The authors think that for the cilia this threshold is not met. Thus, the authors emphasize within the long abstract of the manuscript that the CT measurements provide a similar level of detail as the corresponding histological light microscopy images, e.g. page 2, lines 45-46 'Thereby, soft-tissue morphology with a similar detail level as the corresponding histological light microscopy images is reproduced.' To that extent the authors have also revised the sentence on page 3, lines 95-98 'A comparative analysis of the nanoCT slices with corresponding histological light microscopy images confirms the reproduction of the same tissue architecture on a microscopic level in 2D, enabling histopathological characterization of the tissue sample.' to 'A comparative analysis of the nanoCT slices with corresponding histological light microscopy images confirms the reproduction of tissue architecture with similar detail on a microscopic level in 2D, enabling histopathological characterization of the tissue sample.' Furthermore, the difference has been stated in the caption of Figure 3 (page 9, 358-361) '(b) Minimum intensity projection slice derived from the same nanoCT data set shown in (a) with a virtual slice thickness of approximately 7 µm, which allows for clear visualization of the cell nuclei. (c) Representative histological section displaying thick ascending limbs of the loop of Henle with clear visualization of cell nuclei and brush border.'

The samples are wedged inside of a tube rather than in a solid medium such as paraffin,

with saturated ethanol to theoretically keep the sample from shrinkage. A picture of this arrangement and an indication of the purposes of details of the design, in the figure legend, would be valuable, alongside representation in the video protocol.

The authors thank the reviewer for the statement concerning the mounting of the soft-tissue sample in an appropriate sample holder. The first aspect asks for an explanation why the sample is not embedded in a solid medium such as paraffin and instead stored in a tube above 70% (v/v) ethanol. Considering the sample movement, the embedding in paraffin might look beneficial. However, the preparation of the paraffin block limits the user in the size of the sample, which can be investigated. Secondly, the authors wanted to minimize further impacts on the sample. To embed the soft-tissue sample in paraffin, several steps including a dehydration series in ethanol and often immersion in isopropanol must be performed. Followed by immersion in xylol and infiltration of the paraffin overnight. This might affect the overall image quality with respect to CT. Despite that, the ability to measure the sample in a 'hydrated state' is rather seen as an advantage over other techniques that need embedding of the sample, which as described above for histopathology involves several chemical steps.

The second aspect concerns the design of the sample holder. Here, the authors wanted to simply provide an example how that sample holder could look like. Therefore, the authors write in the manuscript (page 4, line 167) 'In case of the stained mouse kidney: …', which follows the general actions for this specific protocol step (page 4, lines 165-167) 'Mount the soft-tissue sample to an appropriate sample holder. Ensure a tight fit of the sample on the sample holder to prevent the sample from moving during the X-ray CT measurements.' Thus, the user is free to decide on the design, which enables the user to accommodate the specific needs concerning their samples and instruments (The sample holder area in a microCT scanner varies between instruments, which would result in a different sample holder design.). An important requirement is that the sample must keep its position within the sample holder during the measurement. As this specific protocol step is part of the video protocol, the authors do not think that a specific figure is needed here.

Ethanol can be associated with shrinkage and sample movement during a scan could cause resolution problems. A paragraph addressing these concerns, along with explanations of chosen imaging parameters such as projection acquisition time could be beneficial to a new audience.

The authors acknowledge the concern of the reviewer with respect to shrinkage associated with ethanol. However, the authors have not observed any shrinkage of the sample – especially with reference to the high-resolution microCT scan, which

lasted several hours, the sample stayed intact during the CT measurements. As the soft-tissue sample has to be kept moist at all times, otherwise the sample is affected severely due to degradation artifacts, the solvent ethanol seems a good choice as it is also the dehydration solvent used later in the preparation for further investigations in histopathology and with the nanoCT. The authors have added an extra sentence to the notes of the specific protocol step 2.1 (page 5, lines 181-182) 'It should be noted that shrinkage artifacts due to the solvent ethanol were not observed.' Additionally, the authors have included a sentence with the desired information in the discussion (page 10, lines 411-412) 'Shrinkage artifacts due to the solvent ethanol, which was used to keep the sample moist during the microCT measurements, were not observed.'

As to the acquisition parameters, the authors have stated the acquisition parameters used in case of the stained mouse kidney in the protocol, e.g. the specific protocol step 2.1 (page 5, lines 187-188) 'In case of the presented microCT data: Acquire the scan at a peak voltage of 50 kV, a current of 3.5W using 1601 projections equally distributed over 360°.' and (page 5, lines 190-197) 'Note: The acquisition parameters for the overview CT scan were chosen for best image quality. As such the 0.39x camera objective was chosen to cover the whole sample within the field of view (FOV). This resulted in an effective pixel size of 12 µm. The exposure time of 2 s per projection provided a good signal to noise ratio. The ROI for the high-resolution CT scan was identified using the microCT data from the overview scan. MicroCT scanners often incorporate an integrated software tool, which allows for the precise selection of the determined ROI. For the high-resolution CT data, the 4x camera objective was chosen resulting in an effective pixel size of 3.3 µm. Here, an exposure time of 15 s per projection was needed.' As every sample has its own requirements to achieve best image quality, the stated acquisition parameters serve as an example only.

Minor Concerns:

The resolution of the histology pictures is poor. A higher resolution photo would be more appropriate representation of what typical histology looks like.

We acknowledge the comment by the reviewer. The authors provided images with 400 dpi for initial submission. To ensure high resolution throughout production, the authors have submitted each figure as vector image file (.svg) as part of the revised submission.

Lines 159-161 The following sentence is confusing: "The X-ray microCT measurements were performed with an Xradia 500 Versa from Zeiss, 160 which offers next to overview

CT measurements the performance of high-resolution CT measurements down to 1µm." what does "next to overview" mean? What is the point?

We acknowledge the reviewer's concern raising from the statement. With overview scan the authors refer to the possibility to image the whole sample within the FOV. Despite that the microCT used by the authors has two further objectives installed, which enable high-resolution scans allowing to focus in on one area of the sample (Selection of volumes of interest is possible.). Generally, local (higher resolution) CT measurements are possible with voxel sizes down to approximately 1µm next to global (overview or lower resolution) CT measurements. The revised sentence (page 4, lines 160-163) has been rewritten to 'The X-ray microCT measurements were performed with a microCT scanner, which offers next to overview CT measurements (Ability to image the entire sample within the field of view (FOV).) the performance of high-resolution CT measurements (Ability to focus in on one desired volume of interest (VOI) of the very same sample.) down to 1µm.'

Line 230ff Critical Dry Point is unfamiliar to most pathologists who may want to use the procedure. Please explain the reasons for its use and the principles, with citations, in appropriate detail somewhere.

The authors acknowledge the reviewer's suggestion with reference to the CPD methodology. For the nanoCT investigations, which provide the highest resolutions and sub-cellular structural information, smaller tissue pieces retrieved from the original sample were critically point dried (CPD). This has been necessary to ensure that the sample can be mounted to the sample holders of the nanoCT, is not moving during the measurement and can be positioned very close to the X-ray source to allow for best geometrical magnification (The nanoCT setup is based on mere geometrical magnification, which is defined as the distance (source-detector) over distance (sample-source)). The application of CPD enables the complete dehydration of the tissue sample by exchanging the solvent (here ethanol) with the drying agent (here CO_2). This drying technique was first introduced by Anderson (1) to preserve the 3D structure of biological specimens for electron microscopy. An overview of the technique is provided by Bray (2).

(1) Anderson, T. F. Techniques for the preservation of three-dimensional structure in preparing specimens for the electron microscope. *Transactions of the New York Academy of Sciences.* 13, 130–133 (1951).

(2) Bray, D. Critical Point Drying of Biological Specimens for Scanning Electron Microscopy in Supercritical Fluid Methods and Protocols. Methods in Biotechnology, Williams J.R., Clifford A.A. (eds), vol 13., 235-243 (Humana Press, 2000).

As suggested by the reviewer, we added the following paragraph to the specific protocol step 3.1.4 citing the two references listed above (page 6, lines 239-247):

'Note: The application of CPD enables the complete dehydration of the tissue sample by exchanging the solvent (here ethanol) with the drying agent (here CO_2). This has been necessary to ensure that the sample can be mounted to the sample holders of the nanoCT, is not moving during the measurement and can be positioned very close to the X-ray source to allow for best geometrical magnification (The nanoCT setup is based on mere geometrical magnification, with the magnification factor being defined as the source-to-detector distance over the source-to-sample distance). The drying technique was first introduced by Anderson to preserve the 3D structure of biological specimens for electron microscopy[28]. An overview of the technique is provided by Bray[29].'

Line 370 Eosin saturation is not "set". It is a property.

We thank the reviewer for pointing out the importance of precise wording. The sentence on page 9, lines 388-389 '. A limitation is here the maximum solubility of eosin in water, which is set to 30 % (w/v) in an aqueous solution.' has been altered to 'A limitation is here the maximum solubility of eosin in water, which is 30 % (w/v) in an aqueous solution.'

Line 416 What do "diffusion rings" look like as related to histology? How large is "large" for a sample?

The authors thank the reviewer for the questions. The authors have inserted Scheme 1 below to illustrate 'diffusion rings' (red dotted lines) within an object. A diffusion ring is a visual mark that indicates how far the stain has diffused into the object with a certain concentration. Generally, the contrast enhancement within one diffusion ring is homogeneous but can vary between different diffusion rings as illustrated in the scheme. Diffusion rings can occur due to different reasons, e.g. the concentration of the stain is to low, and therefore, staining stops at a certain point causing a diffusion ring. Interactions on molecular level between the stain and the tissue can create a diffusion ring. It should be noted that the scheme is an illustration only. Thus, the concentration gradient e.g. could be also inverted. Not every 'marked zone' within a sample is a diffusion ring. Regarding the stained mouse kidney, the differently contrast enhanced areas within the tissue sample are here attributed to structural differences, which accumulate different amounts of staining agent.

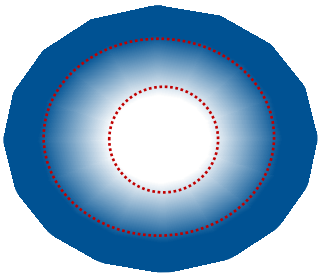

Scheme 1. Illustration of diffusion rings (red dotted lines) within an object. The concentration of the staining agent within one diffusion ring is homogeneously distributed and varies between diffusion rings.

With reference to size, the authors have investigated samples of several centimeters in size. The biggest samples so far had dimensions of (5 cm x 3 cm x 3 cm) and could be completely and homogeneously stained within 24 hours. It should be noted that size is not the only requirement to achieve complete and homogeneous staining. As each specimen is different, the protocol might need adjustment. The authors have emphasized that issue e.g. in the specific protocol step 1.2 on page 4, lines 143-146 'Note: The eosin y staining solution has a concentration of 30 % (w/v) in distilled water. Choose the volume of the staining solution in such a way that the sample is completely covered by the staining solution and allow the sample to move freely within the sample container. The incubation time may differ for other samples and has to be adjusted accordingly.' Additionally, it is addressed in the discussion on page 10, lines 407-409 'It should be noted that the overall staining time and volume of the staining solution needed might request some adaptations depending on the nature of the sample.'